Neurobiology of Disease

Amyloid-β Peptide (Aβ) Neurotoxicity Is Modulated by the Rate of Peptide Aggregation: Aβ Dimers and Trimers Correlate with Neurotoxicity

Lin Wai Hung,[1,2,3,4] Giuseppe D. Ciccotosto,[1,2,4] Eleni Giannakis,[3] Deborah J. Tew,[1,2,4] Keyla Perez,[1,2,4] Colin L. Masters,[2,4] Roberto Cappai,[1,2,4] John D. Wade,[3] and Kevin J. Barnham[1,2,4]

[1]Department of Pathology, [2]Bio21 Molecular Science and Biotechnology Institute, and [3]The Howard Florey Institute of Physiology and Medicine, The University of Melbourne, Parkville, Victoria 3010, Australia, and [4]Mental Health Research Institute, Parkville, Victoria 3052, Australia

Alzheimer's disease is an age-related neurodegenerative disorder with its toxicity linked to the generation of amyloid-β peptide (Aβ). Within the Aβ sequence, there is a systemic repeat of a GxxxG motif, which theoretical studies have suggested may be involved in both peptide aggregation and membrane perturbation, processes that have been implicated in Aβ toxicity. We synthesized modified Aβ peptides, substituting glycine for leucine residues within the GxxxG repeat motif (GSL peptides). These GSL peptides undergo β-sheet and fibril formation at an increased rate compared with wild-type Aβ. The accelerated rate of amyloid fibril formation resulted in a decrease in the presence of small soluble oligomers such as dimeric and trimeric forms of Aβ in solution, as detected by mass spectrometry. This reduction in the presence of small soluble oligomers resulted in reduced binding to lipid membranes and attenuated toxicity for the GSL peptides. The potential role that dimer and trimer species binding to lipid plays in Aβ toxicity was further highlighted when it was observed that annexin V, a protein that inhibits Aβ toxicity, specifically inhibited Aβ dimers from binding to lipid membranes.

Key words: **Alzheimer's disease; amyloid-β; small soluble oligomers; GxxxG; aggregation; neurotoxicity; lipid**

Introduction

Alzheimer's disease (AD) is a degenerative brain disorder that accounts for 50–70% of late-onset dementia (Evans et al., 1989). It is exemplified by the presence of extracellular neuritic (amyloid) plaques and intracellular neurofibrillary tangles (Gorevic et al., 1986). The primary constituent of amyloid plaques are aggregated amyloid-β peptides (Aβ) (Glenner and Wong, 1984; Masters et al., 1985; Joachim et al., 1988). Aβ is a 4 kDa peptide product derived from the amyloid precursor protein (APP) (Selkoe, 2001; Sisodia and St George-Hyslop, 2002) and its generation is closely related to AD pathogenesis (Dudal et al., 2004; Stern et al., 2004; Armstrong, 2006). Recent studies have implicated small soluble oligomers such as dimers, trimers, and dodecamers, which form during Aβ aggregation, as being the main culprits of Aβ toxicity and AD pathogenesis (Walsh et al., 1997, 2002; Hartley et al., 1999; McLean et al., 1999; Rosenblum, 2002; Relini et al., 2004; Walsh and Selkoe, 2004; Lesné et al., 2006).

Given the significant role for Aβ oligomerization in AD pathogenesis, it is important to identify the sequence motifs within Aβ that modulate peptide oligomerization and toxicity. Recent literature has implicated a motif within Aβ as being potentially responsible for the conformational transition that precedes the oligomerization of Aβ (Liu et al., 2005). This motif comprises four glycine residues found within the Aβ 25–37 segment (Fig. 1) and is known as the GxxxG repeat motif. Theoretical studies have indicated that this motif might facilitate the conversion of α-helical or random coiled Aβ to β-sheet and eventually fibril formation (Liu et al., 2005). The GxxxG repeat motif is also thought to be involved in modulating membrane helix–helix interactions (Russ and Engelman, 2000; Kleiger et al., 2002). Munter et al. (2007) demonstrated that transmembrane dimerization of APP has a direct effect on APP processing and specifically implicated the $G_{29}xxxG_{33}$ (Aβ sequence numbers) motif within APP, as playing a significant role in modulating APP dimerization, processing, and Aβ generation (Munter et al., 2007).

The role of the GxxxG motif in Aβ oligomerization and toxicity was investigated using glycine-substituted-to-leucine (GSL) peptides (Fig. 1). These GSL peptides have single amino acid alterations at the respective glycine residues. Biophysical characterization of these GSL peptides suggest that alterations within the GxxxG repeat motif increase the rate of fibril formation, leading to a decrease in the concentration in solution of small soluble oligomers, particularly dimers and trimers. Furthermore, a reduction in the ability of these oligomers to bind to lipid membranes was observed. The differential membrane binding ability of the different Aβ dimers correlates well with the toxicity of their respective peptides. This critical role of dimers in Aβ toxicity was confirmed with annexin V. The capacity of annexin V to reduce

Received Aug. 18, 2008; revised Sept. 22, 2008; accepted Sept. 22, 2008.

This work was supported in part by the National Health and Medical Research Council of Australia and the Australia Research Council.

Correspondence should be addressed to Kevin J. Barnham, Level 4, Bio21 Institute, 30 Flemington Road, Parkville, Victoria 3010, Australia. E-mail: kbarnham@unimelb.edu.au.

DOI:10.1523/JNEUROSCI.3916-08.2008

 0270-6474/08/2811950-09$15.00/0

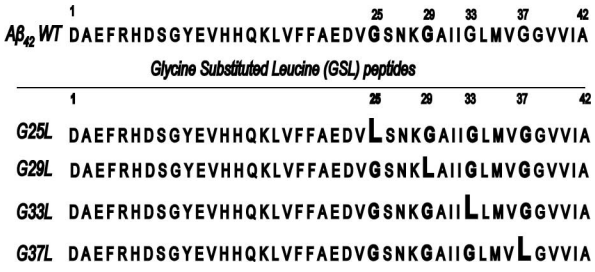

Figure 1. Sequence of Aβ peptides: WT and GSL peptides.

dimer binding to synthetic membranes correlates to its ability to inhibit Aβ toxicity (Lee et al., 2002).

Materials and Methods

Materials

N^{α}-Fmoc-L-OH amino acids, DMF (*N*,*N*-dimethylformamide), and HBTU [2-(1*H*-benzotriazole-1-yl)-1,1,3,3-tetramethyluroniumhexafluoro-phosphate] were purchased from Auspep. DIEA (*N*,*N*-diisopropylethylamine) and HPLC-grade piperidine were purchased from Merck. Resin, Fmoc-L-Ala-PEG-PS was purchased from Applied Biosystems. TES (triethylsilane), hexafluoroisopropanol (HFIP), trifluoroacetic acid (TFA), and DBU (1,8-dizabicyclo[5.4.0]undec-7-ene) were purchased from Sigma-Aldrich. All solvents used were of synthesis grade.

Methods

Peptide synthesis. Continuous-flow Fmoc-SPPS (solid-phase peptide synthesis) was used for all syntheses. $A\beta_{42}$ and the GSL peptides were synthesized on a 0.1 mmol scale using Fmoc-L-Ala-PEG-PS resin as a solid support on an Applied Biosystems Pioneer Synthesizer as described previously (Tickler et al., 2001). GSL peptides were synthesized using the same method as wild-type (WT) Aβ, with single amino acid substitution of glycine to leucine residues in the GxxxG repeat motif. G25L, G29L, G33L, and G37L had leucine replacements at position 25, 29, 33, and 37, respectively.

Preparation and incubation/aggregation of Aβ peptides. Aβ peptides were dissolved in HFIP at a concentration of 1 mg/ml (w/v) to induce a monomeric and helical conformation of the peptides (Smith et al., 2006) Aliquots of 100 μl were dried under vacuum. Dried samples were stored at −20°C.

Samples used for analysis were prepared in the following way: 100 μg aliquots of peptides were dissolved in 50 μl of 20 mM NaOH (w/v) at pH 11 and sonicated for 15 min. After this, the sample was dissolved in 50 μl of 10 mM phosphate buffer (PB) (w/v) at pH 7.4 (10 mM Na_2HPO_4 and NaH_2P0_4) and 400 μl of milliQ H_2O. The solution was filtered using 20 μm Minisart RC4 filters (Sartorius) to ensure preformed aggregates >20 μm were removed. The peptide concentration in solution was determined using a combination of amino acid analysis and spectrophotometric methods. The calculated molar extinction coefficient values of WT, G25L, G29L, G33L, and G37L were 144,999, 167,142, 143,588, 180,000, and 191,605 $L \cdot mol^{-1} \cdot cm^{-1}$, respectively, when using the absorbance value of 214 nm. This was performed to account for any loss of peptide caused by the removal of aggregated material during filtration. Samples were diluted to 10 μM (w/v) and incubated at 37°C shaking at 1400 rpm to induce fibril formation. Incubated samples were measured for various static parameters.

Thioflavin T binding assay for the generation of amyloidogenic structures. A kinetic aggregation assay was performed using the "Simple read" program on a Varian Cary Eclipse Fluorescence Spectrophotometer (Smith et al., 2006). Aβ peptides, prepared as described above, were diluted in 10 mM PB, pH 7.4 to a final concentration of 10 μM with thioflavin T (ThT) to 20 μM. Excitation and emission wavelength were at 444 and 480 nm, respectively. Excitation and emission slit widths were both at 5 nm. The photomultiplier was set to 680 V. The signal was normalized by subtracting the signal with buffer containing ThT alone and dividing by the maximum signal seen with WT Aβ.

Far UV circular dichroism spectroscopy. Circular dichroism (CD) spectroscopy was performed on a Jasco J815 CD spectropolarimeter. Measurements were performed in the far UV with the CD signal being recorded in a 0.1 cm path length Helma quartz cuvette. Investigation of secondary structure during aggregation was performed at a protein concentration of 10 μM (w/v) (Smith et al., 2006). A composite buffer containing 1 mM PB (w/v), 2 mM NaOH (w/v) at pH 7.4 was used in all measurements. Measurements were recorded at 37°C from 185 to 260 nm with a 1 nm bandwidth, 0.1 nm resolution, interval speed of 500 nm/min, and a response time of 1 s. Peptide measurements were subtracted from background readings to give a normalized spectrum. Spectra were converted from machine units in millidegrees, to delta epsilons (Lobley et al., 2002). After delta epsilon conversion, deconvolution of the resulting spectra was achieved using a CDSSTR analysis program provided in the Dichroweb database (Lobley et al., 2002). Using this program, the relative amounts of random coil, α-helix, β-sheet, and β-turn were determined from the normalized contribution of each secondary structure element function to the observed spectrum after curve fitting.

Primary neuronal cultures. Mouse cortical neuronal cultures were prepared as described previously under sterile conditions (Barnham et al., 2003; Ciccotosto et al., 2004). Briefly, embryonic day 14 BL6J×129sv mouse cortices were removed, dissected free of meninges, and dissociated in 0.025% (w/v) trypsin in Krebs' buffer. The dissociated cells were triturated using a filter-plugged fine pipette tip, pelleted, resuspended in plating medium (minimum Eagle's medium, 10% fetal calf serum, 5% horse serum), and counted. Cortical neuronal cells were plated into poly-D-lysine-coated 48-well plates at a density of 150,000 cells/well in plating medium. All cultures were maintained in an incubator set at 37°C with 5% CO_2. After 2 h, the plating medium was replaced with fresh Neurobasal medium containing B27 supplements, geneticin, and 0.5 mM glutamine (all tissue culture reagents were purchased from Invitrogen unless otherwise stated). This method resulted in cultures highly enriched for neurons (>95% purity) with minimal astrocyte and microglial contamination, as determined by immunostaining of culture preparations using specific marker antibodies (data not shown).

Cell viability assays. The neuronal cells were allowed to mature for 6 d in culture before commencing treatment using freshly prepared Neurobasal medium plus B27 supplements minus antioxidants. For the treatment of neuronal cultures, freshly prepared soluble Aβ stock solutions were diluted to the final concentration in Neurobasal medium. The mixtures were then added to neuronal cells for up to 4 d *in vitro*. Cell survival was monitored by phase contrast microscopy, and cell viability was quantitated using the 3-(4,5-dimethylthiazol-2-yl)-5-(3-carboxymethoxyphenyl)-2-(4-sulfophenyl)-2*H*-tetrazolium) or MTS assay, as described previously (Ciccotosto et al., 2004). Briefly, the medium was replaced with fresh Neurobasal medium supplemented with B27 lacking antioxidants and 10% v/v MTS (Promega) was added to each well and incubated for 3 h at 37°C in a 5% CO_2 incubator. Plates were gently shaken, and a 150 μl aliquot from each well was transferred to separate wells of a 96-well plate. The color change of each well was determined by measuring the absorbance at 490 nm using a PerkinElmer Wallac Victor Multireader, and background readings of MTS incubated in cell-free medium were subtracted from each value before calculations. The data were normalized and calculated as a percentage of untreated vehicle control values. Vehicle control in this study consists of 4 mM NaOH in PBS buffer.

Surface enhanced laser desorption/ionization–time of flight–mass spectrometry. Surface enhanced laser desorption/ionization–mass spectrometry (SELDI-MS) experiments were performed on H50 ProteinChip arrays (Bio-Rad), which have a hydrophobic surface comprising six carbon molecules (C6) (Davies et al., 1999).

Detection of oligomers. Arrays were washed twice with 5 μl of 10 mM PB, pH 7.4, on a shaking table for 2 min. PB was then wicked off, and 10 μM peptide samples (prepared as described above) were loaded onto the arrays and allowed to incubate for 2 h, while shaking. Samples were wicked off and arrays were washed twice with PB, followed by two 1 min washes with 1 mM HEPES, pH 7.2. The arrays were air dried and matrix was applied. One microliter of 50% α-cyano-4-hydroxycinnamic acid (CHCA) (w/v) matrix in 50% acetonitrile (v/v) and 0.5% TFA (v/v) was

applied twice to each array with arrays being air dried between each application (Guerreiro et al., 2006). The matrix, which is an energy-absorbing molecule, facilitates desorption and ionization of peptides in the MS. Arrays were then analyzed by surface enhanced laser desorption/ionization–time of flight–mass spectrometry (SELDI-TOF MS), and resulting spectra were examined using ProteinChip software, version 3.2.1. Various oligomeric forms of the peptides based on the time of flight detector can be separated according to their mass-to-charge (*m*/*z*) ratio. This translates to a spectral view with peaks representing peptides of different molecular masses. Area under the curve (AUC) of each peak was used to quantify the level of binding for each peptide.

Synthetic lipid binding assay. A novel lipid binding assay was designed to mimic detection of specific oligomers of $A\beta_{42}$ WT and GSL peptides binding to lipid membranes. Liposomes [small unilamellar vesicles (SUVs)] were prepared as described below. Arrays were initially washed with 5 μl of 30 mg/ml CHAPS (3-[(3-cholamidopropyl)dimethylammonio]-1-propanesulfonate) (w/v) and immediately wicked off. This was followed by three washes with 5 μl of 10 mM PB on a shaking table for 2 min. After washing, 5 μl of liposomes at 20 mM were placed onto the arrays forming a monolayer of lipids. Control arrays had PB on the hydrophobic surface instead of lipid. Arrays were incubated at 37°C for 2 h to allow for sufficient binding of lipid onto the hydrophobic surface of the chip. The arrays was washed with 10 mM PB to remove unbound lipid, and peptide samples at 50 μM were loaded onto the arrays and allowed to incubate for 5 min. Samples were removed, chips were washed with 10 mM PB twice, followed by two 1 min washes with 1 mM HEPES at pH 7.2. The chips were then air dried and 1 μl of 50% CHCA (w/v) in 50% acetonitrile (v/v) and 0.5% TFA (v/v) was applied onto each spot twice with arrays being air dried between each application. Chips were then analyzed by SELDI-TOF MS, and resulting spectra were examined using ProteinChip software, version 3.2.1. Oligomers binding to the surface of either the lipid or the hydrophobic surface (control arrays) can be separated according to their *m*/*z* ratio. AUC for each peptide was used to quantify the level of oligomer binding to either the lipid layer or the H50 surface. The integrity of the lipid layer was determined by using melittin as a positive control and BSA as a negative control.

Annexin inhibition of oligomeric lipid binding. Inhibition of oligomers binding to the lipid coated H50 array in the presence of annexin V was essentially performed as described above. To test whether annexin V altered the lipid binding of Aβ, an equal ratio of annexin V was incubated for 10 min on the lipid surface before the addition of $A\beta_{42}$. All binding experiments were performed in triplicate.

Liposome (SUV) preparation. SUVs were prepared as described previously (Smith et al., 2006). Lipids, 1-palmitoyl-2-oleoyl-*sn*-glycero-3-phospho-choline (POPC) and 1,2-dioleoyl-*sn*-glycero-3-phospho-L-serine (POPS), were dissolved in chloroform and dried. Lipids were resuspended in 10 mM PB with final lipid concentration of 41 mM. Solutions were placed in a 37°C shaker in the presence of acid-washed glass beads for 30–45 min, followed by sonication for 15 min and a freeze–thawing process (five times) using liquid nitrogen. The suspension was extruded through polycarbonate membranes (Nuclepore; 100 nm pore size) on an extruder apparatus (Avanti Polar Lipids) at 37°C.

Results

The GxxxG mutant peptides have reduced neurotoxic activity

To determine whether the GxxxG repeat motif modulates Aβ toxicity, mouse cortical cultures treated with either 15 μM WT or GSL peptide were measured for cell viability by MTS assay. $A\beta_{42}$ WT peptide decreased neuronal cell viability to 41.4 ± 1.7% (Fig. 2). The G25L and G29L peptides were significantly less toxic ($p < 0.05$ and $p < 0.01$, respectively) to neuronal cells exhibiting 72.7 ± 6.8 and 81.2 ± 3.8% cell viability, respectively, whereas G33L and G37L ($p < 0.01$ for both peptides) treated cells exhibited minimal toxicity (95.9 ± 4.0 and 90.9 ± 9.6% cell viability, respectively). A range of assays was performed to ascertain which biophysical properties associated with changes to the GxxxG motif best correlated with the reduced toxicity and cell binding.

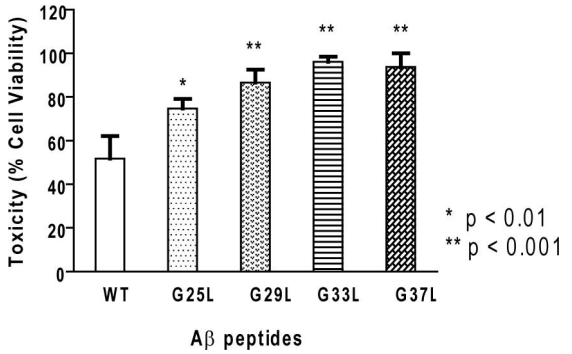

Figure 2. Cell viability assay after treatment with Aβ peptides. Primary cortical neurons were grown at low density (1.25×10^5 cells/cm^2) for 6 d, and the viability of these cells after peptide treatment was determined by measuring the inhibition of MTS reduction. Cortical neurons were treated with 15 μM peptide for 96 h in serum-free media. Results are expressed as percentage of cell viability with mean ± SEM. Cell toxicity assays were done in triplicate and repeated at least three times. A one-way ANOVA using Tukey's multiple-comparison tests comparing WT to other GSL peptides was performed (*$p < 0.01$; **$p < 0.001$).

Time-dependent aggregation profiles of Aβ peptides; GSL peptides have increased rate of β-sheet and fibril formation

Initial ThT measurements of WT $A\beta_{42}$ indicated minimal formation of amyloidogenic material (Fig. 3*A*) at day 0; the ThT signal is expressed as percentage of maximum WT fluorescence. Corresponding EM detected small globular structures on day 0 (supplemental Fig. 1*A*, available at www.jneurosci.org as supplemental material). These structures exhibited diameters ranging from 12 to 24 nm. This was consistent with "pseudospherical" structures as described by Goldsbury et al. (2000). CD spectroscopy indicated that these structures were predominately random coiled (Fig. 3*B*). As incubation time increased, the peptide underwent conformational changes forming predominately β-sheet structures (Fig. 3*C*). After 7 d, there was an extensive network of fibrils (supplemental Fig. 1*D*, available at www.jneurosci.org as supplemental material). The appearance of fibrils correlated with maximum ThT fluorescence (Fig. 3*A*). These results on Aβ amyloid formation are in accordance with previously published studies on Aβ aggregation (Klunk et al., 1989; Jarrett and Lansbury, 1992; Sunde et al., 1997; Kowalewski and Holtzman, 1999; Tjernberg et al., 1999; Kirkitadze et al., 2001).

G25L had similar initial ThT fluorescence to that of the WT peptide; however, differences were observed at later stages of aggregation. Initially, G25L had low initial ThT fluorescence (Fig. 3*A*) and an unordered structure, as indicated by CD spectroscopy (Fig. 3*B*). These structures underwent conformational changes from random coil to β-sheet during the course of aggregation, as indicated by CD spectroscopy (Fig. 3*C*). The increase in β-sheet content of G25L was similar to the WT peptide. However, after a day, there was a sharp increase in ThT fluorescence, which was much more intense than that observed for the WT peptide (Fig. 3*A*), indicating that amyloidogenic material was being generated faster than for WT Aβ. By day 7, there was a network of fibrils observed (supplemental Fig. 2, available at www.jneurosci.org as supplemental material) similar to that of WT. Although the final fibril network is similar to WT, the ThT and CD data indicated that G25L had a much faster rate of aggregation.

The G29L peptide had an aggregation profile similar to that of WT. The ThT fluorescence on day 0 was minimal (Fig. 3*A*). Pseudospherical structures (supplemental Fig. 3*A*, available at www.jneurosci.org as supplemental material) were seen on this day with no ordered structure (Fig. 3*B*). ThT fluorescence grad-

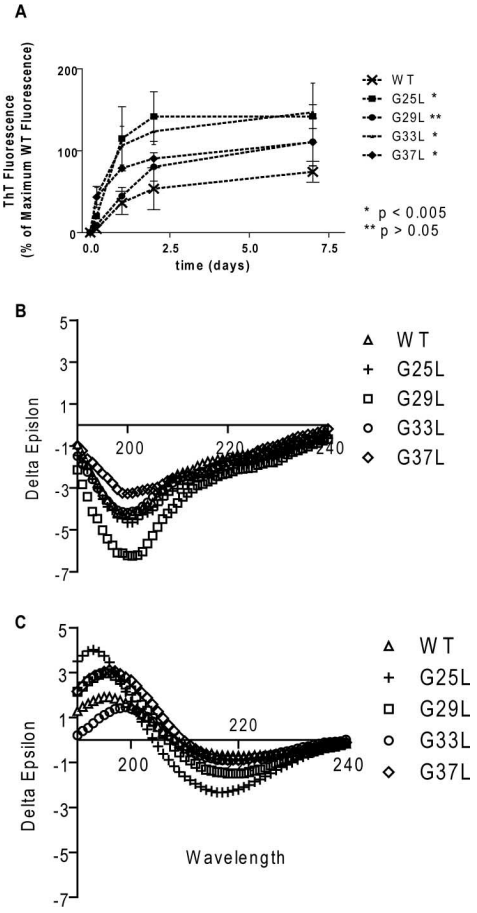

Figure 3. ***A***, Discontinuous ThT fluorescent measurement of $A\beta_{42}$ WT, G25L, G29L, G33L, and G37L ($n = 3$) over a course of 7 d. Fluorescence of peptides is normalized to maximum wild-type fluorescence (100%). Excitation wavelength was 444 nm, whereas emission wavelength is 480 nm. Both excitation and emission slit size was 5 nm. Error bars indicate SEM. Secondary structure transitions of $A\beta_{42}$ peptides at day 0 (***B***) and day 7 (***C***) are shown. ThT and CD assays were done at least three times.

ually increased, reaching a maximum on day 7 (Fig. 3*A*). After 7 d of incubation, fully formed fibrils were present (supplemental Fig. 3*D*, available at www.jneurosci.org as supplemental material). The fibril formation process of G29L was therefore seen to follow a similar trend as WT.

The fibril formation profiles that differ the most from WT were those of G33L and G37L, especially during the initial stages of incubation. Although there was a similar transition of secondary structure from random coil on day 0 to predominately β-sheet thereafter (Fig. 3*B*,*C*), these two peptides had a greater rate of fibril formation as shown in the ThT studies (Fig. 3*A*). This indicated that these peptides underwent rapid fibril formation once in solution. EM studies showed fibrils of a different morphology compared with the WT were detected after 7 d of aging (supplemental Figs. 4, 5, available at www.jneurosci.org as supplemental material) with aggregates showing smaller more branched fibrils than observed for WT Aβ.

Detection of soluble oligomers using SELDI-TOF MS; GSL peptides have reduced concentrations of small soluble oligomers

SELDI-TOF MS is a mass spectroscopy method allowing for detection of oligomers based on their differential molecular weights. The hydrophobic nature of the peptides facilitates their interaction with the carbon molecules on the surface of the H50 ProteinChip array used in this study. Therefore, by using SELDI-TOF MS, the different oligomeric states formed during aggregation of the various Aβ peptides were compared and correlated with toxicity.

In addition to the monomer, this method detected a range of WT oligomeric species, ranging from dimeric species up to octamers (Fig. 4*A*) with the most predominate species present being the dimer when Aβ was aged for a day; a representative complete SELDI-MS TOF spectrum is shown in supplemental Figure 6 (available at www.jneurosci.org as supplemental material). There were distinct differences in the oligomeric profile of the GSL peptides compared with WT Aβ. Although all oligomeric species up to an octamer were detected for the WT, only species up to trimers were detected for the GSL peptides. In addition, there was a reduction in the levels of these oligomers compared with the WT (Fig. 4*B*). The GSL dimers were not as pronounced as that of the WT, with monomer levels being much higher than that of dimers. This indicated that there has been a reduction in the quantity of smaller oligomers for the GSL peptides present in solution compared with the WT.

Aβ aggregation has long been recognized as a necessary condition for toxicity and it has been hypothesized that dimers and trimers of Aβ are the principal toxic species (Podlisny et al., 1995; Roher et al., 1996, 2000; McLean et al., 1999); therefore, we examined whether there was a correlation between the levels of detectable monomer and the various oligomeric species with the toxicity of the respective peptides. The data shown in Figure 4 indicate that there is a negative correlation between the levels of monomer and toxicity ($r^2 = 0.96$; $p = 0.004$) (Fig. 4*C*), whereas there is a highly significant positive correlation between the levels of dimer ($r^2 = 0.8267$; $p < 0.05$) and trimer ($r^2 = 0.996$; $p < 0.0005$) (Fig. 4*D*,*E*) of the various peptides and their respective toxicity levels. In addition, it was observed that a dose-dependent increase in toxicity of Aβ was accompanied by a similar dose–response increase in the percentage of dimers present in the Aβ solution (Fig. 4*F*). At 5 μM, Aβ WT cell viability was 92% with corresponding monomer and dimer levels of 46 and 54%, respectively, whereas at 15 μM, Aβ WT cell viability was at 52% with corresponding monomer and dimer levels at 12 and 87%, respectively. This further demonstrates the crucial role small soluble oligomers may play in Aβ toxicity.

Detection of small oligomers bound to lipid surface by SELDI-TOF MS; GSL have reduced oligomers detected on the lipid membranes

The SELDI-TOF MS method was extended to investigate the interaction of oligomeric species with membrane surfaces because various studies have shown a correlation between lipid interactions and Aβ toxicity (Kayed et al., 2004; Ambroggio et al., 2005).

Detection of oligomeric forms of Aβ peptides on a membrane surface was accomplished using a novel method developed in our laboratory (Giannakis et al., 2008). H50 ProteinChip arrays were coated with liposomes; the carbon molecules on the surface were able to interact with the hydrophobic chains of the lipids via hydrophobic interactions, thereby coating the surface of the chip with a lipid monolayer. Oligomers binding to the lipid surface were then detected by mass spectroscopy. As a positive control, melittin, a bee venom protein that is known to bind to lipid membranes, demonstrated selective binding to the lipid-coated arrays, which confirmed the integrity of the lipid layer, whereas BSA (negative control) showed minimal binding to the lipid sur-

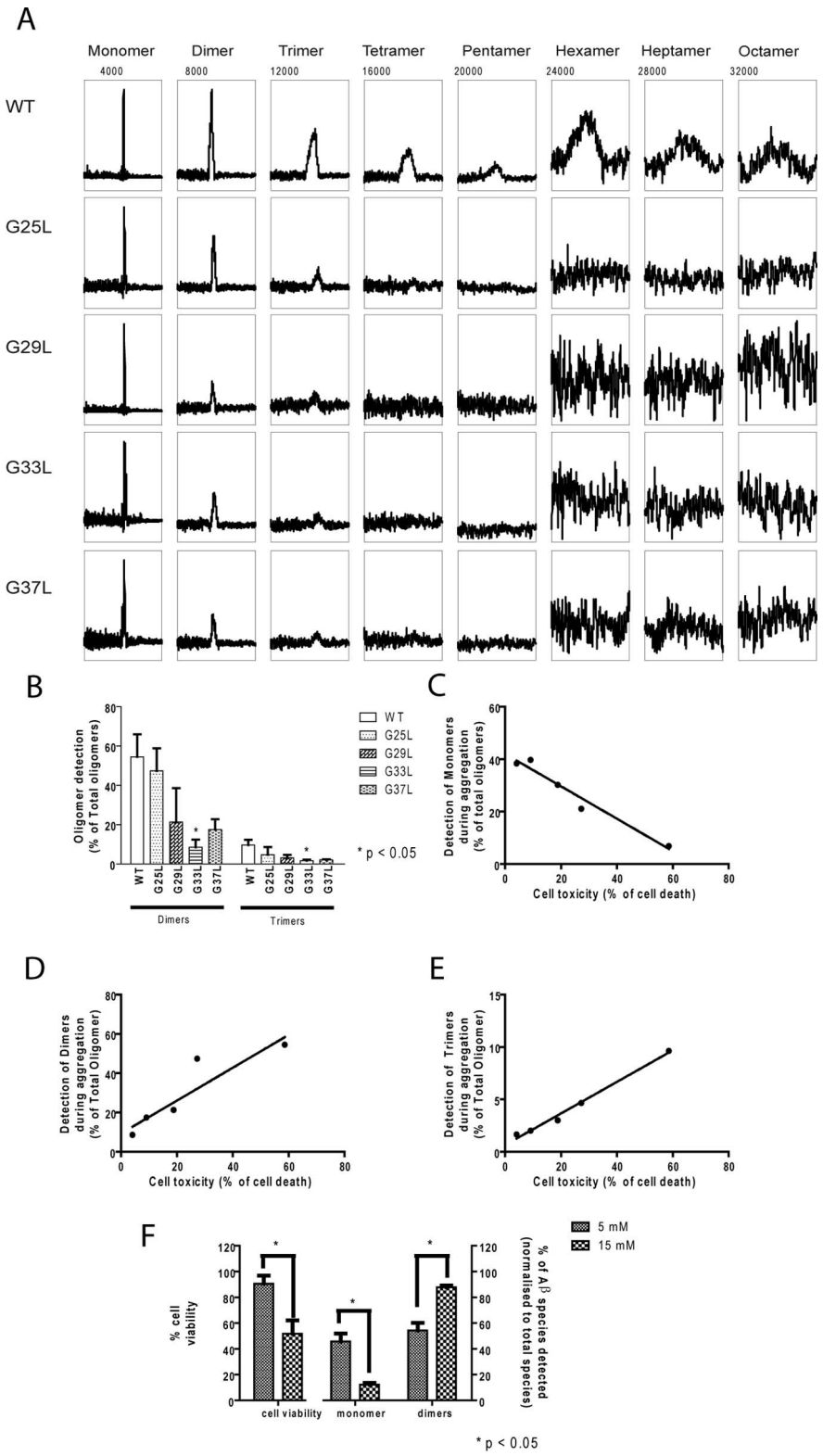

Figure 4. ***A***, Detection of oligomeric Aβ species using SELDI-TOF MS. Oligomeric species up to octamers were detected for WT Aβ. Oligomeric species of up to trimer were observed for G25L, G33L, and G37L peptides. Tetramers were also detected for G29L. ***B***, Areas under the curve of peaks as seen in ***A*** were used to quantify oligomers. The values shown here are expressed as percentage of total oligomeric detection after a day of aging. This assay was performed in duplicates and repeated at least three times. Correlation of the amount of monomer dimer and trimer present with toxicity are shown in ***C–E***, respectively. The quantity of detected oligomers by SELDI-TOF MS after a day of incubation is represented on the *y*-axis and correlated to cell toxicity on the *x*-axis. Statistically significant correlation of monomer ($r^2 = -0.96$; $p = 0.0035$) (***C***), dimer ($r^2 = 0.83$; $p = 0.03$) (***D***), and trimer (***E***) detected during aggregation to toxicity ($r^2 = 0.99$; $p = 0.0004$). ***F***, Graph showing concentration-dependent decrease in cell viability to $A\beta_{42}$ WT. Concentrations of 5 and 15 μM Aβ were used. Similarly, monomers and dimers were also analyzed after a day of incubation using SELDI-TOF MS on a H50 hydrophobic surface at these concentrations. SELDI-TOF MS analysis revealed a similar dose-dependent decrease in the percentage of monomers present in the Aβ solution as well as a concentration-dependent increase in the percentage of dimers. Error bars indicate SEM.

face. The converse was true for the H50 arrays not coated in lipid (Giannakis et al., 2008).

Figure 5 shows the differential binding affinity of the oligomers to the lipid monolayer. For the WT peptide, only monomers, dimers, and trimers could be detected binding to the lipid monolayer (Fig. 5*A*), although mass spectrometry analysis of the peptide in solution indicated that up to octamers were present in solution (Fig. 4*A*). However, assessment of the AUC values revealed only small levels of dimers and trimers of G25L and G29L bound to the lipid monolayer, whereas G33L and G37L peptides had minimal oligomer binding to the lipid with only monomers detected (Fig. 5*C*). Therefore, one of the obvious differences between WT and the GSL peptides is the lipid binding ability of the dimeric species. Whereas predominately dimeric species of WT were detected on the lipid after a day of aging (Fig. 5*B*), there is a significantly lower level of G25L and G29L dimers detected, with minimal binding of G33L and G37L dimers to the lipid surface (Fig. 5*C*).

Given that small soluble oligomers of Aβ have previously been implicated as the toxic species via membrane interactions (Podlisny et al., 1995; Roher et al., 1996, 2000; MacKenzie and Engelman, 1998; McLean et al., 1999; Walsh et al., 2002; Kayed et al., 2004; Tickler et al., 2005; Lesné et al., 2006), the ability of dimer and trimer of each peptide to bind to the lipid, as detected by SELDI-TOF MS, was correlated to toxicity (Fig. 6*B*,*C*). Correlations of dimer and trimer to toxicity gave r^2 values of 0.96 and 0.90, respectively. Furthermore, monomers were seen to be negatively correlated to toxicity ($r^2 = 0.956$; $p = 0.004$) as seen in Figure 6*A*.

Annexin V inhibition of oligomeric lipid binding

Annexin V, which has a high affinity for phosphatidylserine lipid head groups, has previously been shown to inhibit Aβ toxicity by stopping Aβ binding to cell membranes (Lee et al., 2002). To investigate whether annexin V was able to alter the oligomeric profile of Aβ binding to lipid membranes, the binding of oligomeric Aβ

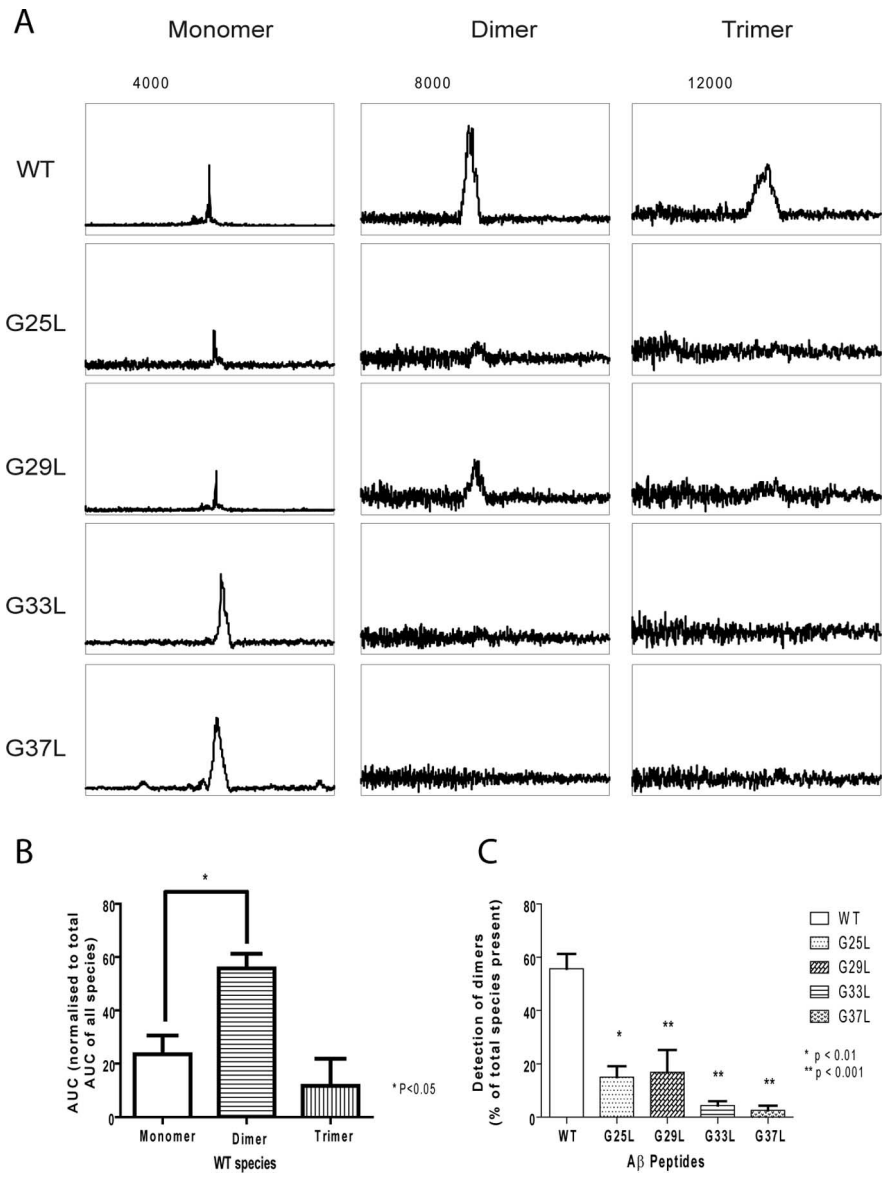

Figure 5. ***A***, Detection of oligomeric Aβ species binding to lipid via SELDI-TOF MS. Oligomeric species up to tetramers could be seen binding to the lipid. Oligomers belonging to G25L and G29L peptides exhibit diminished ability to bind to lipid, whereas no oligomeric species for G33L and G37L were detected on the lipid. Membrane consists of equal ratios of POPC and POPS (20 mM of each lipid). ***B***, Detection of wild-type Aβ oligomers binding to lipid via SELDI-TOF MS. Aβ WT dimeric species are found to be more abundant on the lipid compared with monomeric and trimeric species. ***C***, Dimers of each peptide were compared; dimers of the WT are detected more readily on the lipid surface than the other GSL dimers. Values are quantified using the area under the curve for oligomeric peak obtained by SELDI-TOF MS. The signals are expressed as percentage of total oligomers binding to the lipid after a day of aging. The synthetic lipid binding assay was done in duplicate and repeated at least three times. A one-way ANOVA using Tukey's multiple-comparison tests comparing dimers of WT and GSL peptides was performed (*$p < 0.01$). Error bars indicate SEM.

to lipid membranes as determined by SELDI-TOF MS was repeated in the presence of annexin V. The results shown in Figure 7 indicated that, in the presence of annexin V, there was a large and specific decrease in the amount of dimer and trimer of WT $A\beta_{42}$ bound to the lipid, a 70 and 85% reduction, respectively; however, because of the relatively small amounts of trimer observed, only the reduction in dimer reached statistical significance ($p = 0.009$). Importantly, there was no decrease in the amount of monomer bound to the lipid in the presence of annexin V, implying that the inhibition of dimeric and trimeric Aβ was through inhibiting a specific interaction between the oligomers and the lipid and that the nature of this interaction is different than the interaction that the monomer has with the lipid.

Discussion

Alzheimer's disease is a neurodegenerative disorder that is related to protein misfolding and aggregation. The aggregation process induces fibril formation by Aβ peptides; it is believed that along the aggregation pathway toxic intermediates such as small soluble oligomers are generated (Walsh et al., 2002; Walsh and Selkoe, 2004; Lesné et al., 2006). Because it has been shown in theoretical studies that the GxxxG repeat motif within the Aβ sequence may have a role in fibrillization, investigation of peptides with alterations in this motif may provide insight into how aggregation of Aβ relates to toxic species generation (Liu et al., 2005). In addition, the GxxxG repeat motif has also been implicated in helix–helix interactions in various membrane proteins (Russ and Engelman, 2000).

The GSL peptides used in this study have leucine substitution at respective glycine residues; leucine and not alanine was used to replace the glycine residues because AxxxG and GxxxA motifs have also been implicated in modulating protein/protein interactions (Kleiger et al., 2002). The GSL peptides were seen to undergo a conformational transition to β-sheet and form fibrillar material (Fig. 3). These results do not support the reported theoretical studies undertaken by Liu et al. (2005), who postulated that glycine residues within the GxxxG repeat motif of Aβ facilitated amyloid formation and substitution of these residues would inhibit fibril formation (Liu et al., 2005). Not only were these peptides capable of forming β-sheet fibrils, these peptides formed more fibrils and at a faster rate than the WT. This effect on fibril formation may be attributable to the increase in hydrophobicity; according to the scale of Kyte and Doolittle (1982), replacing a glycine residue with leucine leads to a 0.15 increase in the mean hydrophobicity of the peptide. The effect of hydrophobicity on the rate of peptide aggregation has been previously demonstrated (Calamai et al., 2003; Chiti et al., 2003).

The lack of toxicity seen by these GSL peptides is consistent with literature that shows that some effective inhibitors of Aβ-induced toxicity appear to alter Aβ aggregation by increasing the rate of peptide aggregation (Pallitto et al., 1999). The relationship between rate of aggregation and toxicity shown in this study may have parallels with plaque formation *in vivo*. Amyloid plaques, although being the main pathological marker of AD, do not correlate to disease progression, and it has been postulated that the deposition of plaque is a protective mechanism against the toxicity of soluble Aβ (Cuajungco et al., 2000). Plaque formation

could therefore be a process by which the body attempts to deal with Aβ misfolding and aggregation by partitioning Aβ peptides into nontoxic aggregates via accelerating fibril formation. Indeed, elements that are associated with the plaques such as zinc and neuroserpin are known to accelerate the aggregation of Aβ peptides and have been shown to inhibit Aβ toxicity (Cuajungco et al., 2000; Kinghorn et al., 2006). Results seen here are also consistent with those seen by Cheng et al. (2007) in which transgenic mice carrying the Aβ arctic mutation, which has the propensity to increase Aβ fibrillization, had normal neurological functions, although there was an increase in plaque load (Cheng et al., 2007).

Interestingly, accelerated fibril formation resulted in a decreased ability of these peptides to generate small soluble oligomers. Results obtained from SELDI-TOF MS indicated that these GSL peptides have much lower levels of dimers and trimers than those of WT with minimal presence of "higher order" oligomers (Fig. 4) during the early stages of aggregation. This is consistent with the concentration-dependent toxicity of WT Aβ, which showed an increase in the percentage of oligomers present at higher, more toxic, peptide concentrations (Fig. 4*F*). Hence, there appears to be a relationship between the formation of such small oligomeric species and toxicity with monomer disappearance associated with increased toxicity (Fig. 4*C–E*). This is in accordance with previous studies (Yankner et al., 1989; Stern et al., 2004) that indicated that production of soluble oligomeric intermediates was responsible for Aβ toxicity (Yankner et al., 1989; Stern et al., 2004; Cappai and Barnham, 2007). Such oligomers have been shown to be toxic in CNS slice cultures (Lambert et al., 1998) and inhibited hippocampal long-term potentiation in rats (Walsh et al., 2002). In particular, oligomers of low molecular weight such as dimeric and trimeric forms of Aβ are prime suspects in instigating toxicity. Putative dimers and trimers were detected in the culture media of Chinese hamster ovary cells expressing endogenous or transfected amyloid APP (Podlisny et al., 1995). Likewise, dimers and trimers isolated from AD brain amyloid deposits were able to elicit neuronal death (Roher et al., 1996, 2000; McLean et al., 1999).

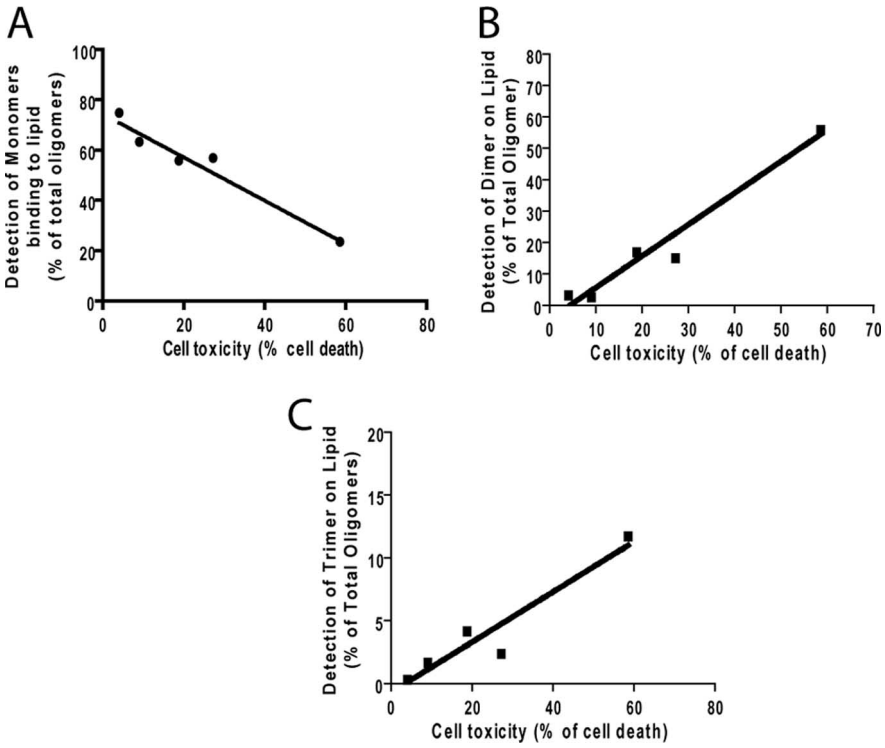

Figure 6. Correlation of membrane binding by monomeric, dimeric, and trimeric species with toxicity. The detection of monomer, dimer, and trimer by SELDI-TOF MS on day 1 are represented on the *y*-axis and correlated to cell toxicity of peptides. Statistically significant correlation of monomer ($r^2 = -0.96$; $p = 0.004$) (***A***), dimer ($r^2 = 0.96$; $p = 0.041$) (***B***), and trimer (***C***) detected on lipid to toxicity ($r^2 = 0.97$; $p = 0.013$).

Because these small oligomers are thought to exhibit their toxic effects through membrane interactions, we extended the SELDI-TOF MS system to investigate the interaction of these oligomers with a lipid surface (Kayed et al., 2004; Tickler et al., 2005; Smith et al., 2006). In this method, a monolayer of lipid was coated onto the surface of a hydrophobic ProteinChip array. Any species interacting with the lipid layer were detected via mass spectroscopy. By using this novel assay, we were able to demonstrate that there is a correlation between peptide toxicity and lipid membrane binding propensity of Aβ dimers and trimers. This is consistent with the concept that Aβ toxicity is manifested via its interaction with neuronal cell membranes (Kayed et al., 2004; Tickler et al., 2005; Smith et al., 2006). Investigating this lipid system, we were only able to detect significant amounts of WT monomeric, dimeric, and trimeric species on the lipid, although there is a much greater range of oligomers present in the sample solution (Fig. 5). WT dimers were the most abundant of all WT species detected on the lipid membrane after a day of incubation (Fig. 5*B*). This is consistent with *in vivo* studies showing that Aβ dimers accumulate in lipid rafts at a time when memory impairment begins in Tg2576 mice (Kawarabayashi et al., 2004). These Aβ dimer levels increase steadily from 6-month-old mice and become the major form of Aβ present in lipid rafts in 11-month-old Tg2576 mice.

A reduction in the amount of detectable oligomers was observed for the GSL peptides on the lipid surface with G33L and G37L having no detectable oligomers on the lipid surface. Therefore, the ability to generate significant quantities of oligomers capable of binding to a lipid membrane correlates with the respective toxicities of the various peptides (Fig. 6*B*,*C*). The negative correlation of monomer to toxicity (Fig. 6*A*) further validates the role of dimers/trimers in Aβ toxicity. This specificity of the dimers/trimers for a role in Aβ toxicity was confirmed with annexin V inhibition of oligomer binding to membranes. Lee et al. (2002) have shown that annexin V is able to inhibit binding of Aβ to lipid membranes by competitively binding to the negatively charged phosphatidylserine (PS) head groups (Lee et al., 2002). This inhibition resulted in attenuated Aβ toxicity (Lee et al., 2002). Moreover, it has been reported that cells with exposed PS were more sensitive to Aβ toxicity than non-PS-exposed cells (Simakova and Arispe, 2007). Annexin V in this study was able to specifically inhibit dimeric and trimeric species of Aβ from binding to a lipid surface with no effect on monomeric levels, suggesting that the dimer/trimer binds to the lipid in a different manner than the monomer. Studies performed by Kayed et al. (2004) showed that binding of soluble oligomers to lipids increased con-

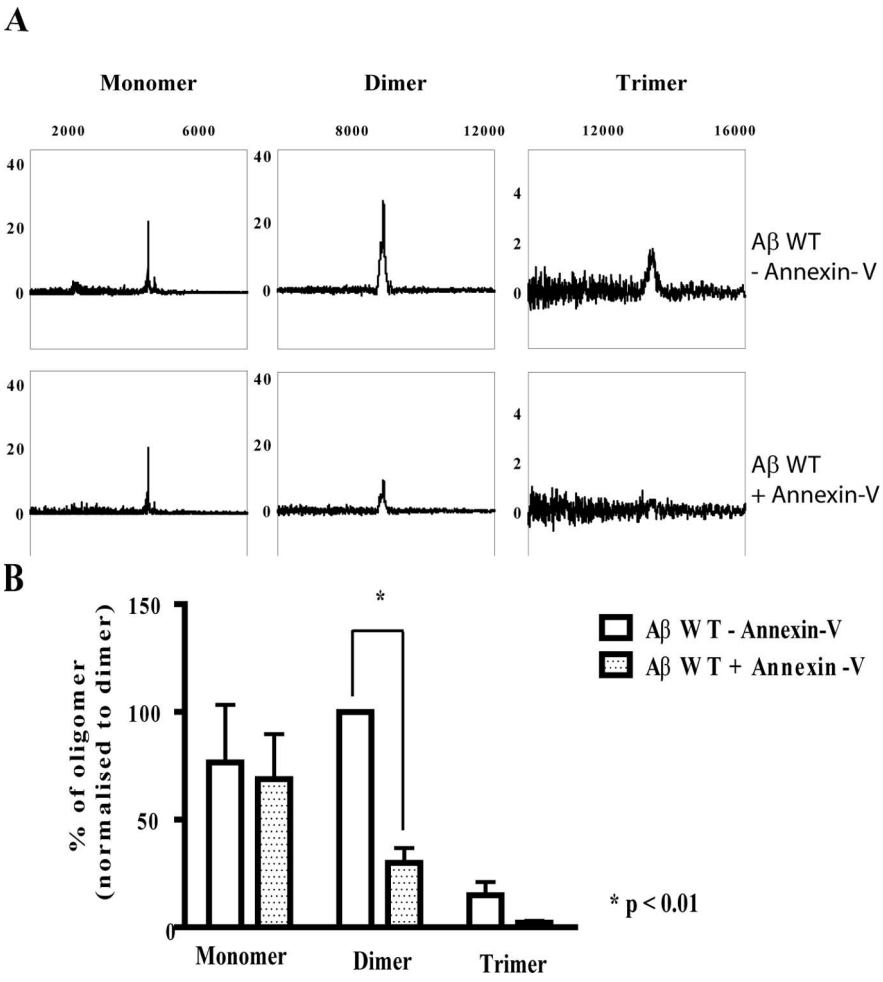

Figure 7. Annexin inhibition of lipid binding by oligomeric Aβ species. Annexin V was incubated on the lipid membrane for 10 min before addition of $A\beta_{42}$ WT. The lipid binding assay is the same as the one described in Figure 5. $A\beta_{42}$ WT was incubated for 1 d shaking at 37°C before addition onto the lipid system. ***A***, SELDI-TOF MS spectra of the monomer, dimer, and trimer with and without the presence of annexin V. ***B***, Values are quantified using the area under the curve for the respective peaks obtained by SELDI-TOF MS. The signals are expressed as percentage of dimer present in the absence of annexin V. This assay was done in duplicate and repeated three times. A paired *t* test was performed comparing the oligomers in the presence and absence of annexin (*$p < 0.01$). Error bars indicate SEM.

ductance across the bilayer membrane (Kayed et al., 2004), an indication of membrane disruption. However, fibrillar Aβ did not have any effect on the membrane conductance, suggesting limited lipid binding by these species.

In conclusion, the GxxxG repeat motif is reported here to modulate the formation of oligomeric species of Aβ. Modification of this motif led to increased rate in amyloid formation. SELDI-TOF MS results showed that increased rate of fibril formation led to a decrease in the formation of toxic oligomeric species. In solution, Aβ peptides exist as inter-converting ensemble of various oligomeric forms, and recent studies have implicated dimers and trimers as the potential toxic species (Shankar et al., 2008); our data provide evidence that is consistent with this literature. The differential pattern of toxicity, oligomeric formation, and lipid binding ability of the GSL peptides along with the specific inhibition of the lipid binding by annexin V implicate dimeric and trimeric species of Aβ interacting with lipid membranes as being key modulators of Aβ toxicity.

References

Ambroggio EE, Kim DH, Separovic F, Barrow CJ, Barnham KJ, Bagatolli LA, Fidelio GD (2005) Surface behavior and lipid interaction of Alzheimer beta-amyloid peptide 1-42: a membrane-disrupting peptide. Biophys J 88:2706–2713.

Armstrong RA (2006) Plaques and tangles and the pathogenesis of Alzheimer's disease. Folia Neuropathol 44:1–11.

Barnham KJ, Ciccotosto GD, Tickler AK, Ali FE, Smith DG, Williamson NA, Lam YH, Carrington D, Tew D, Kocak G, Volitakis I, Separovic F, Barrow CJ, Wade JD, Masters CL, Cherny RA, Curtain CC, Bush AI, Cappai R (2003) Neurotoxic, redox-competent Alzheimer's beta-amyloid is released from lipid membrane by methionine oxidation. J Biol Chem 278:42959–42965.

Calamai M, Taddei N, Stefani M, Ramponi G, Chiti F (2003) Relative influence of hydrophobicity and net charge in the aggregation of two homologous proteins. Biochemistry 42:15078–15083.

Cappai R, Barnham KJ (2007) Molecular determinants of Alzheimer's disease Aβ peptide neurotoxicity. Future Neurology 2:397–409.

Cheng IH, Scearce-Levie K, Legleiter J, Palop JJ, Gerstein H, Bien-Ly N, Puoliväli J, Lesné S, Ashe KH, Muchowski PJ, Mucke L (2007) Accelerating amyloid-beta fibrillization reduces oligomer levels and functional deficits in Alzheimer disease mouse models. J Biol Chem 282:23818–23828.

Chiti F, Stefani M, Taddei N, Ramponi G, Dobson CM (2003) Rationalization of the effects of mutations on peptide and protein aggregation rates. Nature 424:805–808.

Ciccotosto GD, Tew D, Curtain CC, Smith D, Carrington D, Masters CL, Bush AI, Cherny RA, Cappai R, Barnham KJ (2004) Enhanced toxicity and cellular binding of a modified amyloid beta peptide with a methionine to valine substitution. J Biol Chem 279:42528–42534.

Cuajungco MP, Goldstein LE, Nunomura A, Smith MA, Lim JT, Atwood CS, Huang X, Farrag YW, Perry G, Bush AI (2000) Evidence that the beta-amyloid plaques of Alzheimer's disease represent the redox-silencing and entombment of abeta by zinc. J Biol Chem 275:19439–19442.

Davies H, Lomas L, Austen B (1999) Profiling of amyloid beta peptide variants using SELDI Protein Chip arrays. Biotechniques 27:1258–1261.

Dudal S, Krzywkowski P, Paquette J, Morissette C, Lacombe D, Tremblay P, Gervais F (2004) Inflammation occurs early during the Abeta deposition process in TgCRND8 mice. Neurobiol Aging 25:861–871.

Evans DA, Funkenstein HH, Albert MS, Scherr PA, Cook NR, Chown MJ, Hebert LE, Hennekens CH, Taylor JO (1989) Prevalence of Alzheimer's disease in a community population of older persons. Higher than previously reported. JAMA 262:2551–2556.

Giannakis E, Pacífico J, Smith DP, Hung LW, Masters CL, Cappai R, Wade JD, Barnham KJ (2008) Dimeric structures of alpha-synuclein bind preferentially to lipid membranes. Biochim Biophys Acta 1778:1112–1119.

Glenner GG, Wong CW (1984) Alzheimer's disease: initial report of the purification and characterization of a novel cerebrovascular amyloid protein. Biochem Biophys Res Commun 120:885–890.

Goldsbury CS, Wirtz S, Müller SA, Sunderji S, Wicki P, Aebi U, Frey P (2000) Studies on the in vitro assembly of Aβ 1-40: implications for the search for Aβ fibril formation inhibitors. J Struct Biol 130:217–231.

Gorevic PD, Goñi F, Pons-Estel B, Alvarez F, Peress NS, Frangione B (1986) Isolation and partial characterization of neurofibrillary tangles and amyloid plaque core in Alzheimer's disease: immunohistological studies. J Neuropathol Exp Neurol 45:647–664.

Guerreiro N, Gomez-Mancilla B, Charmont S (2006) Optimization and

evaluation of surface-enhanced laser-desorption/ionization time-of-flight mass spectrometry for protein profiling of cerebrospinal fluid. Proteome Sci 4:7.

Hartley DM, Walsh DM, Ye CP, Diehl T, Vasquez S, Vassilev PM, Teplow DB, Selkoe DJ (1999) Protofibrillar intermediates of amyloid β-protein induce acute electrophysiological changes and progressive neurotoxicity in cortical neurons. J Neurosci 19:8876–8884.

Jarrett JT, Lansbury PT Jr (1992) Amyloid fibril formation requires a chemically discriminating nucleation event: studies of an amyloidogenic sequence from the bacterial protein OsmB. Biochemistry 31:12345–12352.

Joachim CL, Morris JH, Selkoe DJ (1988) Clinically diagnosed Alzheimer's disease: autopsy results in 150 cases. Ann Neurol 24:50–56.

Kawarabayashi T, Shoji M, Younkin LH, Wen-Lang L, Dickson DW, Murakami T, Matsubara E, Abe K, Ashe KH, Younkin SG (2004) Dimeric amyloid β protein rapidly accumulates in lipid rafts followed by apolipoprotein E and phosphorylated tau accumulation in the Tg2576 mouse model of Alzheimer's disease. J Neurosci 24:3801–3809.

Kayed R, Sokolov Y, Edmonds B, McIntire TM, Milton SC, Hall JE, Glabe CG (2004) Permeabilization of lipid bilayers is a common conformation-dependent activity of soluble amyloid oligomers in protein misfolding diseases. J Biol Chem 279:46363–46366.

Kinghorn KJ, Crowther DC, Sharp LK, Nerelius C, Davis RL, Chang HT, Green C, Gubb DC, Johansson J, Lomas DA (2006) Neuroserpin binds Abeta and is a neuroprotective component of amyloid plaques in Alzheimer disease. J Biol Chem 281:29268–29277.

Kirkitadze MD, Condron MM, Teplow DB (2001) Identification and characterization of key kinetic intermediates in amyloid beta-protein fibrillogenesis. J Mol Biol 312:1103–1119.

Kleiger G, Grothe R, Mallick P, Eisenberg D (2002) GXXXG and AXXXA: common alpha-helical interaction motifs in proteins, particularly in extremophiles. Biochemistry 41:5990–5997.

Klunk WE, Pettegrew JW, Abraham DJ (1989) Quantitative evaluation of congo red binding to amyloid-like proteins with a beta-pleated sheet conformation. J Histochem Cytochem 37:1273–1281.

Kowalewski T, Holtzman DM (1999) In situ atomic force microscopy study of Alzheimer's beta-amyloid peptide on different substrates: new insights into mechanism of beta-sheet formation. Proc Natl Acad Sci U S A 96:3688–3693.

Kyte J, Doolittle RF (1982) A simple method for displaying the hydropathic character of a protein. J Mol Biol 157:105–132.

Lambert MP, Barlow AK, Chromy BA, Edwards C, Freed R, Liosatos M, Morgan TE, Rozovsky I, Trommer B, Viola KL, Wals P, Zhang C, Finch CE, Krafft GA, Klein WL (1998) Diffusible, nonfibrillar ligands derived from Abeta1–42 are potent central nervous system neurotoxins. Proc Natl Acad Sci U S A 95:6448–6453.

Lee G, Pollard HB, Arispe N (2002) Annexin 5 and apolipoprotein E2 protect against Alzheimer's amyloid-beta-peptide cytotoxicity by competitive inhibition at a common phosphatidylserine interaction site. Peptides 23:1249–1263.

Lesné S, Koh MT, Kotilinek L, Kayed R, Glabe CG, Yang A, Gallagher M, Ashe KH (2006) A specific amyloid-beta protein assembly in the brain impairs memory. Nature 440:352–357.

Liu W, Crocker E, Zhang W, Elliott JI, Luy B, Li H, Aimoto S, Smith SO (2005) Structural role of glycine in amyloid fibrils formed from transmembrane alpha-helices. Biochemistry 44:3591–3597.

Lobley A, Whitmore L, Wallace BA (2002) DICHROWEB: an interactive website for the analysis of protein secondary structure from circular dichroism spectra. Bioinformatics 18:211–212.

MacKenzie KR, Engelman DM (1998) Structure-based prediction of the stability of transmembrane helix-helix interactions: the sequence dependence of glycophorin A dimerization. Proc Natl Acad Sci U S A 95:3583–3590.

Masters CL, Simms G, Weinman NA, Multhaup G, McDonald BL, Beyreuther K (1985) Amyloid plaque core protein in Alzheimer disease and Down syndrome. Proc Natl Acad Sci U S A 82:4245–4249.

McLean CA, Cherny RA, Fraser FW, Fuller SJ, Smith MJ, Beyreuther K, Bush AI, Masters CL (1999) Soluble pool of Abeta amyloid as a determinant of severity of neurodegeneration in Alzheimer's disease. Ann Neurol 46:860–866.

Munter LM, Voigt P, Harmeier A, Kaden D, Gottschalk KE, Weise C, Pipkorn R, Schaefer M, Langosch D, Multhaup G (2007) GxxxG motifs within the amyloid precursor protein transmembrane sequence are critical for the etiology of Abeta42. EMBO J 26:1702–1712.

Pallitto MM, Ghanta J, Heinzelman P, Kiessling LL, Murphy RM (1999) Recognition sequence design for peptidyl modulators of beta-amyloid aggregation and toxicity. Biochemistry 38:3570–3578.

Podlisny MB, Ostaszewski BL, Squazzo SL, Koo EH, Rydell RE, Teplow DB, Selkoe DJ (1995) Aggregation of secreted amyloid beta-protein into sodium dodecyl sulfate-stable oligomers in cell culture. J Biol Chem 270:9564–9570.

Relini A, Torrassa S, Rolandi R, Gliozzi A, Rosano C, Canale C, Bolognesi M, Plakoutsi G, Bucciantini M, Chiti F, Stefani M (2004) Monitoring the process of HypF fibrillization and liposome permeabilization by protofibrils. J Mol Biol 338:943–957.

Roher AE, Chaney MO, Kuo YM, Webster SD, Stine WB, Haverkamp LJ, Woods AS, Cotter RJ, Tuohy JM, Krafft GA, Bonnell BS, Emmerling MR (1996) Morphology and toxicity of Abeta-(1–42) dimer derived from neuritic and vascular amyloid deposits of Alzheimer's disease. J Biol Chem 271:20631–20635.

Roher AE, Baudry J, Chaney MO, Kuo YM, Stine WB, Emmerling MR (2000) Oligomerizaiton and fibril asssembly of the amyloid-beta protein. Biochim Biophys Acta 1502:31–43.

Rosenblum WI (2002) Structure and location of amyloid beta peptide chains and arrays in Alzheimer's disease: new findings require reevaluation of the amyloid hypothesis and of tests of the hypothesis. Neurobiol Aging 23:225–230.

Russ WP, Engelman DM (2000) The GxxxG motif: a framework for transmembrane helix-helix association. J Mol Biol 296:911–919.

Selkoe DJ (2001) Alzheimer's disease: genes, proteins, and therapy. Physiol Rev 81:741–766.

Shankar GM, Li S, Mehta TH, Garcia-Munoz A, Shepardson NE, Smith I, Brett FM, Farrell MA, Rowan MJ, Lemere CA, Regan CM, Walsh DM, Sabatini BL, Selkoe DJ (2008) Amyloid-beta protein dimers isolated directly from Alzheimer's brains impair synaptic plasticity and memory. Nat Med 14:837–842.

Simakova O, Arispe NJ (2007) The cell-selective neurotoxicity of the Alzheimer's Aβ peptide is determined by surface phosphatidylserine and cytosolic ATP levels. Membrane binding is required for Aβ toxicity. J Neurosci 27:13719–13729.

Sisodia SS, St George-Hyslop PH (2002) gamma-Secretase, Notch, Abeta and Alzheimer's disease: where do the presenilins fit in? Nat Rev Neurosci 3:281–290.

Smith DP, Smith DG, Curtain CC, Boas JF, Pilbrow JR, Ciccotosto GD, Lau TL, Tew DJ, Perez K, Wade JD, Bush AI, Drew SC, Separovic F, Masters CL, Cappai R, Barnham KJ (2006) Copper-mediated amyloid-beta toxicity is associated with an intermolecular histidine bridge. J Biol Chem 281:15145–15154.

Stern EA, Bacskai BJ, Hickey GA, Attenello FJ, Lombardo JA, Hyman BT (2004) Cortical synaptic integration *in vivo* is disrupted by amyloid-β plaques. J Neurosci 24:4535–4540.

Sunde M, Serpell LC, Bartlam M, Fraser PE, Pepys MB, Blake CC (1997) Common core structure of amyloid fibrils by synchrotron X-ray diffraction. J Mol Biol 273:729–739.

Tickler AK, Barrow CJ, Wade JD (2001) Improved preparation of amyloid-beta peptides using DBU as Nalpha-Fmoc deprotection reagent. J Pept Sci 7:488–494.

Tickler AK, Smith DG, Ciccotosto GD, Tew DJ, Curtain CC, Carrington D, Masters CL, Bush AI, Cherny RA, Cappai R, Wade JD, Barnham KJ (2005) Methylation of the imidazole side chains of the Alzheimer disease amyloid-beta peptide results in abolition of superoxide dismutase-like structures and inhibition of neurotoxicity. J Biol Chem 280:13355–13363.

Tjernberg LO, Callaway DJ, Tjernberg A, Hahne S, Lilliehöök C, Terenius L, Thyberg J, Nordstedt C (1999) A molecular model of Alzheimer amyloid beta-peptide fibril formation. J Biol Chem 274:12619–12625.

Walsh DM, Selkoe DJ (2004) Oligomers on the brain: the emerging role of soluble protein aggregates in neurodegeneration. Protein Pept Lett 11:213–228.

Walsh DM, Lomakin A, Benedek GB, Condron MM, Teplow DB (1997) Amyloid beta-protein fibrillogenesis. Detection of a protofibrillar intermediate. J Biol Chem 272:22364–22372.

Walsh DM, Klyubin I, Fadeeva JV, Cullen WK, Anwyl R, Wolfe MS, Rowan MJ, Selkoe DJ (2002) Naturally secreted oligomers of amyloid beta protein potently inhibit hippocampal long-term potentiation in vivo. Nature 416:535–539.

Yankner BA, Dawes LR, Fisher S, Villa-Komaroff L, Oster-Granite ML, Neve RL (1989) Neurotoxicity of a fragment of the amyloid precursor associated with Alzheimer's disease. Science 245:417–420.